Energy and Buildings 93 (2015) 249–258

Contents lists available at ScienceDirect

Energy and Buildings

journal homepage: www.elsevier.com/locate/enbuild

The joint influence of albedo and insulation on roof performance: An observational study

P. Ramamurthy[a,b], T. Sun[c], K. Rule[d], E. Bou-Zeid[b,*]

[a] Department of Mechanical Engineering, The City College of New York, New York, NY 10031, United States
[b] Department of Civil and Environmental Engineering, Princeton University, Princeton, NJ 08544, United States
[c] Department of Hydraulic Engineering, Tsinghua University, Beijing 100084, China
[d] Princeton Plasma Physics Laboratory, Princeton, NJ 08540, United States

ARTICLE INFO

Article history:
Received 17 December 2014
Received in revised form 14 February 2015
Accepted 16 February 2015
Available online 23 February 2015

Keywords:
Cool roof
Roof albedo
Roof heat flux
Roof insulation

ABSTRACT

This article focuses on understanding the temperature and heat flux fields in building roofs, and how they are modulated by the interacting influences of albedo and insulation at annual, seasonal and diurnal scales. High precision heat flux plates and thermocouples were installed over multiple rooftops of varying insulation thickness and albedo in the Northeastern United States to monitor the temperature and the heat flux into and out of the roof structures for a whole year. Our analysis shows that while membrane reflectivity (albedo) plays a dominant role in reducing the heat conducted inward through the roof structures during the warmer months, insulation thickness becomes the main roof attribute in preventing heat loss from the buildings during colder months. On a diurnal scale, the thermal state of the white roof structures fluctuated little compared to black roof structures; membrane temperature over white roofs ranged between 10 °C and 45 °C during summer months compared to black membranes that ranged between 10 °C and 80 °C. Insulation thickness, apart from reducing the heat conducted through the roof structure, also delayed the transfer of heat, owing to the thermal inertia of the insulation layer. This has important implications for determining the peak heating and cooling times.

© 2015 Elsevier B.V. All rights reserved.

1. Introduction

According to a recent report by the US Department Of Energy [1], the US buildings sector accounted for nearly 41% of national primary energy consumption (i.e. about 7% of the primary energy consumption of the whole world) and almost half of this fraction was used for space heating/cooling. These numbers underline the large share of worldwide energy that is consumed for building air conditioning and suggest that even moderate savings in building energy consumption could go a long way in advancing the world towards future energy sustainability.

Given their large contribution to total building heating and cooling energy consumption [1,2], roofs are increasingly the focus of current research and development efforts. Newer concepts in roof design such as cool (highly reflective) roofs [3–5] and green roofs [6] are being explored by various researchers. These designs, apart from improving the energy efficiency of the buildings, would also have a significant impact on the urban microclimate when implemented at a sufficiently large scale over a given city [7]. While these efforts have underlined the importance of roofs and the potential of their retrofits in decreasing building energy consumption and improving the urban microclimate at various locations, few studies have (a) included measurements inside the roof insulation layers to understand the effect of the roofs' thermal inertia, (b) combined measurement and modeling methodologies with thorough model validation at multiple levels, or (c) examined in-depth the interacting roles of roof albedo (averaged reflectivity) and insulation thickness in reducing heat fluxes through the roof structure. In addition, many studies treat roof structures as homogeneous entities with fixed physical and thermal properties [8]. But real-roofs are composed of membranes, insulators, decks and other elements, each with their own unique attributes. These simplified approaches, while adequate to provide estimates of the impact of certain roof designs on building energy efficiency, are not suitable for probing the thermal dynamics in complex, vertically-heterogeneous, roof structures, or for asserting how local climatology influences optimal roof design.

One consequence of the residual knowledge gap is that for large parts of the US, there are yet no clear and conclusive recommendations as to whether white or black roof are more efficient

* Corresponding author. Tel.: +1 609 258 5429.
E-mail addresses: ebouzeid@princeton.edu, rprathap@gmail.com (E. Bou-Zeid).

http://dx.doi.org/10.1016/j.enbuild.2015.02.040
0378-7788/© 2015 Elsevier B.V. All rights reserved.

Table 1
Building and roof information.

Building name/rooftop elevation	Year of construction	Roof color, R-value ($m^2\,K\,W^{-1}$) at sensor location, year of last retrofit
Admin (ADMw-R8.4) (3.3 m AGL)	1962	White, R8.4 (US unit R48), 2005
Theory (THYb-R3.7) (3.18 m AGL)	1978	Black, R3.7 (US unit R21), 2002
Lyman Spitzer (LSBb-R4.2) (13.38 m AGL)	1992	Black, R4.2 (US unit R24), 2012
Lyman Spitzer (LSBw-R4.2) (13.38 m AGL)	1992	White, R4.2 (US unit R24), 2012
Engineering (EGRb-R6.3) (8.88 m AGL)	1990	Black, R6.3 (US unit R36), 2009

over the course of whole year. As such, there is clearly much that remains to be learned about the thermal dynamics in roof layers and how they affect building performance. Furthermore, there is urgency in filling these knowledge gaps in light of the increasing attention given recently to building energy savings. In the US for example, the Department of Energy has recently created through a $120 million grant the "Energy Efficient Buildings Hub" (http://www.eebhub.org); this work is in fact, and for full-disclosure, part of a project funded by that hub.

A number of recent studies have focused on retrofitting old buildings with newer roofs that have a higher reflectivity membrane and a sound insulation layer [9–12]. The modern roof structures used in such retrofits or in new buildings typically consist of a membrane on top, one or more insulation layers (plywood, fiber board, PolyIso (polyisocyanurate), polystyrene foam) underneath, and a concrete or steel roof deck at the bottom. All these materials have varying physical and thermodynamic properties that modulate the heat transfer through the roof. The membranes are usually thinner and are coated either black or white, which directly affects the albedo [1,13]. The insulation layer beneath the membranes has low thermal conductivity [3,4,14] and low heat capacity, enabling it to reduce the transfer of heat to/from the building and also extending the life of the membrane layer above it. The insulation layers, apart from restricting the transfer of heat by means of low thermal conductivity k ($W\,m^{-1}\,K^{-1}$), also delay the transfer towards the indoor space due to their thermal inertia or effusivity $(k\rho c)^{1/2}$, where ρ ($kg\,m^{-3}$) is the insulation material density and c ($J\,K^{-1}\,kg^{-1}$) is the specific heat capacity. The thermal effusivity is a measure of a material's ability to exchange thermal energy with its surroundings. While the inherent thermal properties restrict the transfer of heat/cold in/out of the buildings, aging reduces the thermal efficiency of the membranes and insulation foams. Natural weathering and accumulation of dust particles decrease the albedo of cool roof membranes [5,15,16] and the inert gas that occupies the cell structure of most PolyIso foams diffuses out and gets replaced by air, thereby increasing the foams thermal conductivity and reducing its heat transfer resistivity [6,17,18]. These effects, combined with the heterogeneous roof structures, complicate sensing and modeling of such roofs.

In this paper, our focus is on experimentally investigating roof structures as heterogeneous entities to elucidate the effects of thermal inertia and albedo on their efficiency in regulating heat transfer into buildings. Of particular interest is the covariance of the effects related to these two roofs parameters: insulation thickness and albedo. To accomplish these aims, we will analyze heat flux and temperature observations at various levels inside different roof elements, and combine them with measurements of atmospheric forcings to study the performance of roof structures.

2. Methodology

The test site for this study was the Princeton Plasma Physics Lab (PPPL) in Princeton, New Jersey, USA (N40.3489° W74.6029°). PPPL consists of a block of interconnected buildings of various heights, built during different time periods. The naming convention, building's respective age, and the roof heights above ground level (AGL) are detailed in Table 1. The table also gives the R-value, which is a measure of the total thermal resistance of the roof insulation: $R = d/k$, where d is the insulation depth and k is the thermal conductivity of the roof. The SI unit of R is $m^2\,K\,W^{-1}$; the table also lists (within braces) the R-value in the more commonly used units in the US, which is $h\,ft^2\,°F\,BTU^{-1}$. Note that the SI R-value ($m^2\,K\,W^{-1}$) = 5.71 R-value ($h\,ft^2\,°F\,BTU^{-1}$).

Fig. 1 shows the plan view of the buildings at PPPL and the markings indicate the locations of our heat flux plate, thermocouple, and weather station installations (detailed later). LSB is a four-story commercial office building. The roof membranes and the insulation foams were newly installed in Summer 2012. Apart from the PolyIso foam, a layer of Densdeck was added between the membrane and the PolyIso. For the specific purposes of this study, a black EPDM membrane was installed over half of the test roof, while the other half was covered with a white EPDM membrane. Both parts were manufactured by Carlisle Technology and installed in the same way; the sensors were embedded at points with identical R-values (the R-value is typically not homogeneous over a roof; it varies horizontally to allow a tapered surface that enhances water drainage). The EGR building, mostly utilized for office space, had a roofing structure that also includes plywood insulation between the top membrane and the insulating PolyIso foam. The last two sites were on top of the ADM and THY building. Both sites contained no additional layers apart from the membrane and the foam. It is important to note (see Table 1) that all the sites varied in either their R-values or their albedos. From here on, the roof installations would be referred by their respective building names, followed by 'b' or 'w' to indicate the membrane color, and then hyphenated by their corresponding R-values.

All data were logged with Campbell Scientific CR 1000 loggers; measurements were sampled at 1 Hz but averaged and outputted every 1 min. Type-T thermocouples (TC) by OMEGA Engineering made from "Special Limits of Error Wire" with glass-braded insulation of the junction were used everywhere. The accuracy, computed following the recommended approach of the data logger manufacturer and with the parameters provided by TC manufacturer (depends on many parameters such as the temperature at the reference junction and the measurement junction) under the experimental condition was estimated to be better than ±0.1 K. A subset of the TCs were also compared in the lab before deployment over a range of temperatures and showed maximum differences between the sensors of less than 0.2 K (confirming a precision of also ±0.1 K). High-performance heat flux plates from Hukseflux, the PU22 model, which is 3 mm thick and 50 mm in diameter (sensitive area is a 20 × 20 mm square), were used. The manufacturer specified relative accuracy is±5%. The inter-plate comparison conducted in the lab on a subset of the heat flux plates and suggested differences between the plates that are smaller than ±5%. The more relevant finding from these tests is that a standard heat flux plate that is typically used for soil measurements (Hukseflux model HFP 01) was also evaluated and showed much larger errors (up to about 7 $W\,m^{-2}$). This underlines the importance of using these high-accuracy thin plates in roof applications where the measured fluxes can be very small and errors related to plate storage and other factors can become important. This is in agreement with the

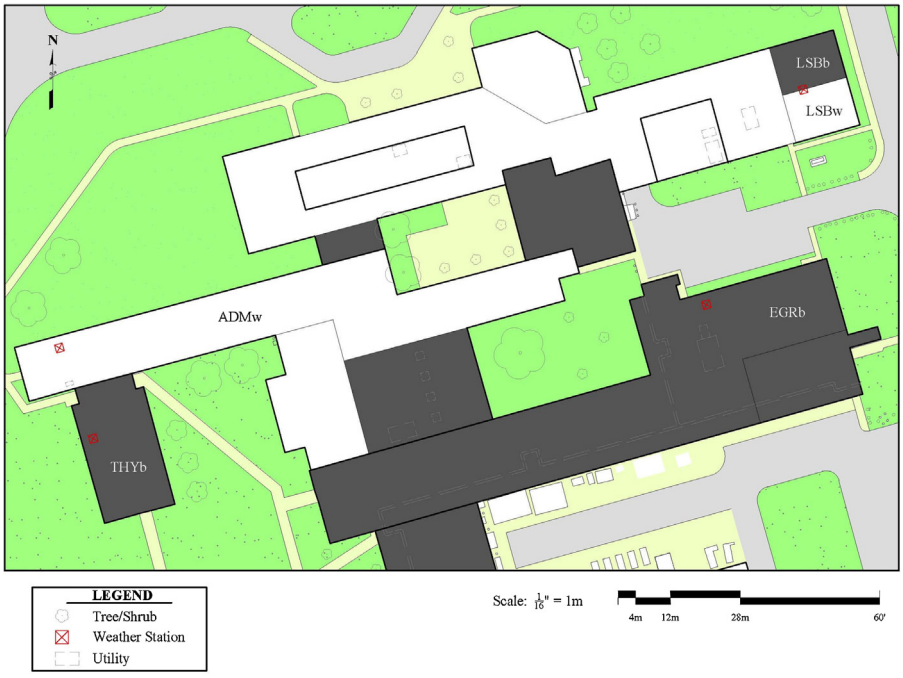

Fig. 1. Map illustrating the buildings and roof installation at PPPL test site. The sensors inside the roof layers were placed very close to installed automated weather stations, but at a sufficient distance to the south of the stations that ensured the roofs over the sensors were not shaded by the weather stations.

Table 2
Roof installation.

Roof	Membrane (mm)	Insulation	Deck
Admin (ADMw-R8.4)	White, 1.5	20.3 cm PolyIso Foam	Concrete
Theory (THYb-R3.7)	Black, 1.5	8.9 cm PolyIso Foam	Corrugated metal
Lyman Spitzer (LSBb-R4.2)	Black, 1.5	1.6 cm Densdeck + 8.9 cm PolyIso Foam	Corrugated metal
Lyman Spitzer (LSBw-R4.2)	White, 3.7	1.6 cm Densdeck + 8.9 cm PolyIso Foam	Corrugated metal
Engineering (EGRb-R6.3)	Black, 2.3	1.3 cm Wood + 13.4 cm PolyIso Foam	Corrugated metal

recommendations of Meyn and Oke [19], who also found that thin plates are needed for building applications under some conditions.

Five thermocouples and two heat flux plates were installed on each roof, except in the ADMw-R8.4 roof where three heat flux plates were used. A roof installation example from the engineering building is shown in Fig. 2 and the details of the membrane and insulation layers for all roofs are provided in Table 2. The depths below the outer surface where the heat flux plates and thermocouples were installed are detailed in Table 3. At all sites, a thermocouple was installed underneath the membrane, another in the middle of the insulation foam, and a third at the interface of building insulation and roof deck; a fourth thermocouple was fixed to the underside of the building deck and a fifth was installed in the air plenum. The heat flux plates were installed underneath the membrane and between the insulation foam and the roof deck; in the admin building (ADM) an additional plate was installed close to the middle of the insulation layer. At all sites, the roof deck was either concrete or corrugated steel. The plates and sensors at the interface of the insulation and deck were installed at the metal-insulation interface (rather than the air-insulation interface).

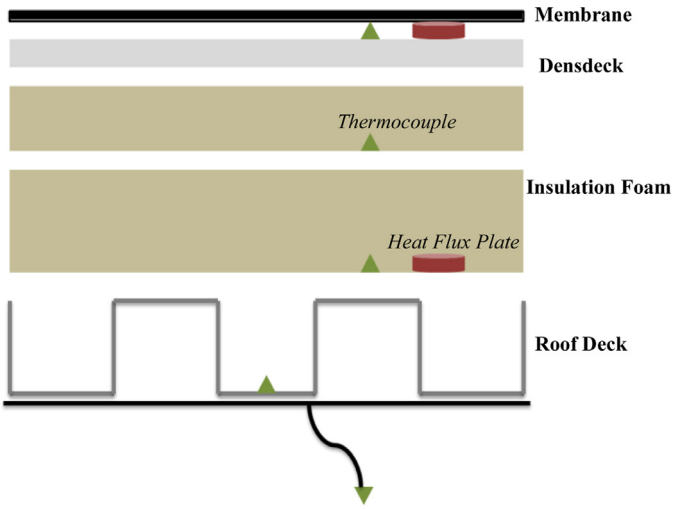

Fig. 2. An illustration of heat flux plate and thermocouple installation at PPPL—from the engineering building (the white spaces in between the layers are not air gaps, but are included in the figure for clarity of illustration).

Table 3
Thermocouple and heat flux plate installation depths. The table lists the depths of the upper three thermocouples (*4 for EGRb). The lowest two thermocouples were installed at the lower surface of the roof deck (pasted to the surface) and in the underlying air plenum. At EGR no thermocouple was installed on the lower roof deck surface.

Roof	Thermocouple installation depths (cm from roof surface)	Heat flux plates installation depths (cm from roof surface)
ADMw-R8.4	0.2, 10.3, 20.5	0.2, 10.3, 20.5
THYb-R3.7	0.2, 4.6, 9.0	0.2, 9.0
LSBb-R4.2	0.2, 5.6, 10.7	0.2, 10.7
LSBw-R4.2	0.4, 5.8, 10.9	0.4, 10.9
EGRb-R6.3	0.2, 1.5, 5.3, 14.8*	0.2, 14.8

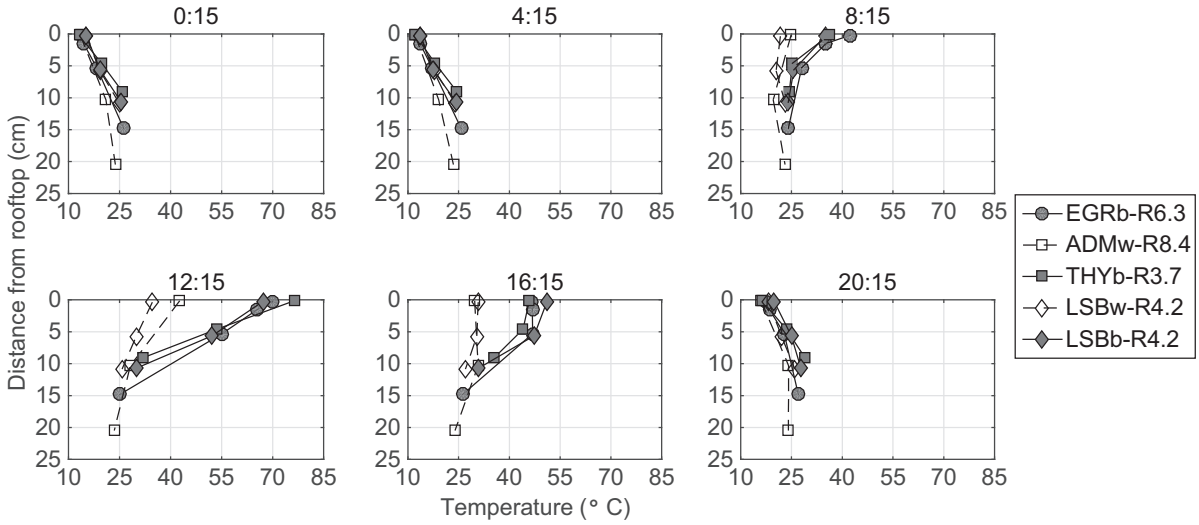

Fig. 3. Monthly-averaged temperature profiles at specific times over various roof structures for August 2012, time is EDT (note that black roof markers are filled in gray and white roof markers are unfilled/white).

Apart from the thermocouple and the heat flux plates, the ambient weather conditions were monitored using wireless Sensorscope® stations (http://www.sensorscope.ch/ [20], see details of all sensors specifically deployed on the stations used here in [21]). These mobile meteorological towers, each 2 m tall, were placed next to the roof installations at all the sites but were not shading the roof over the embedded sensors. In addition to the ambient weather conditions, these instruments monitored surface temperature and albedo.

While combinations of thermocouples and heat flux plates have been previously used to estimate the storage flux in urban areas including roofs before [8,19], and also to test different roofing elements under laboratory conditions [9–11,22,23], our study is unique in the extensive monitoring of 5 roofs that vary both in insulation and albedo at a single site (same meteorological conditions). The comparison of LSB white and black roofs, which are exactly identical in age, construction, and design, is also a critical feature of this study.

The experimental data collection started in late July of 2012 and is ongoing; here we use data from August 2012 to July 2013. It should be noted that there weren't any extended periods when the incident weather was abnormal. The heat flux plates sampled data at 1-min resolution and were checked for erroneous data points and spikes.

3. Results

The collected data were analyzed to understand the effect of insulation *R*-value and roof albedo on heat fluxes into the deck. As noted before, four of the decks consisted of corrugated metal that offered no further resistance to heat flux and hence fluxes at the bottom of the insulation layer are essentially the fluxes into the indoor space. The administration building (ADMw-R8.4) had a concrete deck. But to be able to compare the five sites in a consistent manner, we will ignore the additional resistance this concrete deck offers and simply compare fluxes at the bottom of the insulation layers. It should however be noted that this concrete deck will have a significant influence on the heat entering the building. A focus of our study is to understand how the albedo and *R*-value effects interact. To illustrate such interaction with a simple example, one can consider a very highly insulated roof, say R-40; it is obvious that the albedo of such a roof has no impact on building energy consumption since almost no heat flux will reach the bottom of the insulation. In more practical cases, with an *R*-value less than 9, the effect of the albedo will increase as the *R* decreases and the theoretical maximum albedo effect occurs when $R = 0$.

3.1. Summer temperature and heat flux profiles

Fig. 3 depicts profiles of temperature inside the five roof structures for various times of the day, where each profile is the average of all the individual profiles occurring at that time during August 2012. That is, the figure describes the evolution of temperature over an average August day inside various roof structures. The timestamps shown in Fig. 3 are in EDT (UTC-0400). The zero level in the profiles refers to the top of the roof, just underneath the membrane and the depth then increases, as we get closer to the building's roof deck. The top most value represents the temperature directly underneath the roof's EPDM membrane and the bottom measurement denotes the temperature at the interface of insulation foam and roof deck. The measurements inside the building are omitted since they are not affected by the time of day in the same way as external temperatures (due to air conditioning) are and would confuse the reader. In general these two internal temperatures were similar and did not fluctuate much during a typical day.

During the night and early morning hours (0015 and 0415), the temperature underneath the membrane is around 13–15 °C and it keeps increasing, as we get closer to the roof deck; these low temperatures are the result of cooling of the surface by longwave radiation emission and are lower than external air temperatures, which averaged around 19 °C in August 2012. During this period, the temperature at the air plenum for all the rooftops was around 23–25 °C on average. The structure of the temperature profiles during these late night and early morning hours thus clearly indicate a negative heat transfer, i.e., energy lost from the buildings to the surroundings. This allows the buildings to cool down at night. An important feature to underline is that, during night, the outer surface temperatures are the same over the white and black roofs. This is expected since albedo plays no role at night, and the emissivities of the two roofs are about equal.

However, around 0815 local time, as incoming solar radiation starts increasing, the black roofs transition and start absorbing significant amounts of thermal energy. In contrast, the highly reflective ADMw-R8.4 and LSBw-R4.2 roofs are slower to react. One interesting phenomenon to note during this time period (0815) occurs over the ADMw-R8.4; the insulation element or temperature

sensor at the third depth is at a lower temperature compared to the roof deck below it and the membrane above it. This minimum is expected to occur since the heat flux at the upper surface starts inverting the temperature profiles inside the roof leading to a point where the slope changes sign. At the ADMw-R8.4, which is the most insulated, the difference between depth 1 and 2 and depth 2 and 3 is around 5 °C.

During the midday period, the temperature profiles are completely reversed; the membrane temperature is higher than that of the roof deck. The black roofs are about 30 °C warmer than the white roofs at the outer surface: all three black roofs have membrane temperatures around 65–75 °C, whereas the white roofs ADMw-R8.4 and LSBw-R4.2 have temperatures of 42 °C and 35 °C, respectively. A second transition occurs during the evening period, around 1615 local time, when the roofs begin to cool. Their surface temperatures being very elevated, they now radiate, convect, and reflect more energy than they receive despite the fact that shortwave solar radiation is still quite significant at that time. As expected, the black roofs cool faster between 1215 and 1615: the black roof membrane temperatures drop by almost 30 °C compared to a 10 °C observed drop for the white membranes.

At night, around 2015 local time, the temperature profiles are reversed again. The membranes become cooler than the roof decks as the surface continues to lose heat to the surrounding environment by radiation. During this time period though, the temperature at depth 3 was higher than the temperature at the deck and plenum (not shown here) for all the sites indicating that outward heat flux from the building, which was observed at 0015 starts later at night.

The profiles of temperature inside the roof structures clearly illustrate the periodicity of the thermal dynamics at play during the warmer month. All five roof structures, irrespective of their albedo and insulation thickness, transition from a heat source for the indoor space during the day to a heat sink for the indoor space at night. However, the magnitude of the shift and the heat sources and sinks the indoor space experiences clearly depend on the albedo and the insulation thickness of the roof structures. The insulation was also found to cause a phase shift (delay) in heat transfer due to its thermal inertia, leading to maxima and minima in the temperature profiles occurring inside the roof layers at various times; thicker insulation naturally produced larger shifts.

This section of the analysis will focus on how the temperature profiles discussed above get translated to heat fluxes, but unlike the five levels of temperature measurements, the heat flux plates were only installed at two levels due mainly to their high cost. Recall that these two levels are at the top of the roof, underneath the membrane, and at the bottom, at the interface between roof insulation and the solid deck. ADMw-R8.4 had one extra heat flux plate towards the middle.

Fig. 4 shows averaged profiles of heat flux inside five roof structures (same *y*-axis scale as Fig. 3). These are also the averaged fluxes, at those times, over all the days of August 2012. As expected from the temperature profiles, at night, there is a net negative heat flux indicating loss of energy from the buildings; however, it is important to note that more energy is lost from the top membrane layer compared to the bottom. The differences between top and bottom fluxes are 0.6–1.3 W m^{-2}, with the more insulated roof structures losing less heat at the bottom compared to the relatively thin insulated structures. However, the fluxes versus depth profiles collapse suggesting that the lower bottom losses in the thicker roofs are directly attributable to the higher thermal inertial of these roofs (surface cooling takes longer to be felt at larger depths). At 0415, while the structure of the heat flux profile remains identical to that of 0015, the magnitude of heat loss increases slightly despite the fact that surface temperature are not significantly different; this increase in surface cooling might be related to the atmospheric cooling and the concomitant reduction in downwelling longwave radiation. During the morning transition period, while the bottom heat flux remains slightly negative (∼−1.5 W m^{-2}) at all sites, the exterior surfaces actively absorb incoming solar radiation producing a downward (positive) heat flux at the top. At EGRb-R6.3 for example, while the heat flux at the bottom is −0.6 W m^{-2}, the membrane absorbs nearly 40 W m^{-2}. The temperature of all surface rise considerable as illustrated previously in Fig. 3.

As the surface temperatures rise, the roofs start losing larger heat fluxes by radiative and convective transfer to the atmosphere. Therefore, by 1215 local time, the net heat fluxes at the top decrease considerably, and for EGRb-R6.3 they even switch to net heat losses at the top; all other roof structures continue to actively absorb heat but at lower magnitudes than in the early morning. This quick transition observed at EGRb-R6.3 is related to the low thermal capacity of the plywood underlying the membrane, which is used as a secondary insulation layer separating the membrane from the PolyIso foam. The low heat capacity implies lower thermal inertia, which results in rapid responses of EGRb-R6.3: it heats fast (highest surface temperature at 0815) and then switches regime the earliest.

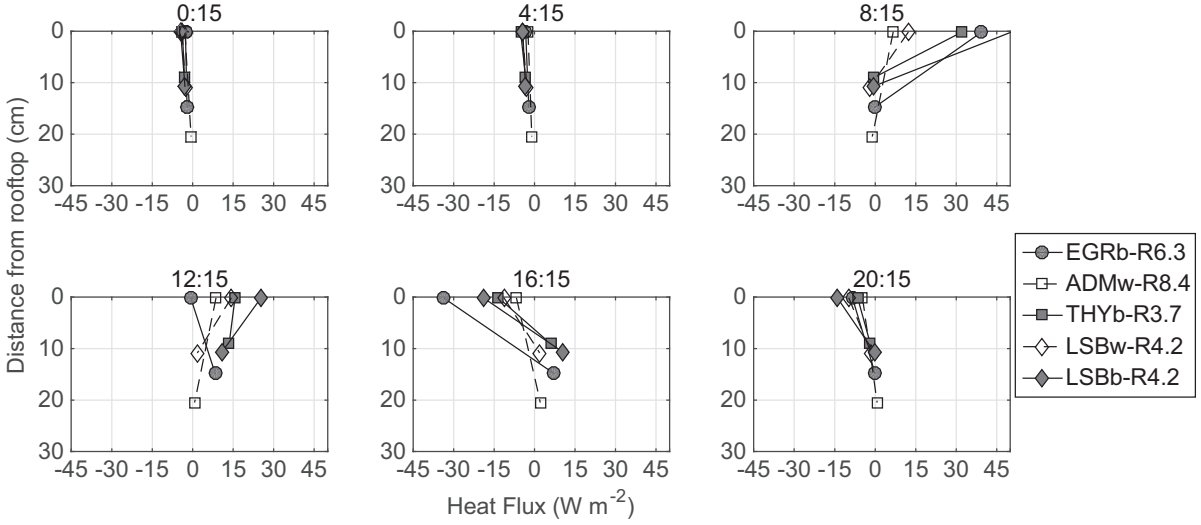

Fig. 4. Averaged heat flux profiles over different roof structures for August 2012; times in EDT (note that black roof markers are filled in gray and white roof markers are unfilled/white).

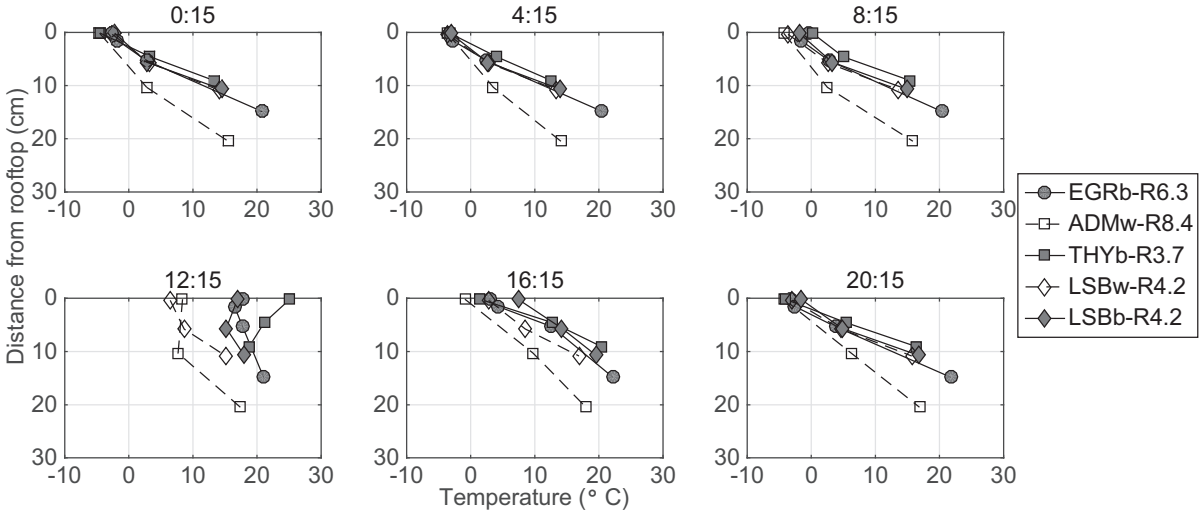

Fig. 5. Averaged temperature profiles over different roofs for January 2013.

Over all roof structures, the fluxes at the bottom are positive (into the building) at 1215, but the black roofs clearly conduct higher fluxes into the indoor space.

At 1615, the top of the insulation layer cools down and releases heat into the atmosphere over all roofs; however, the bottom parts are still conducting the heat stored inside the roof layers into the buildings. By nighttime (2015), while the bottom layers cool down substantially (bottom heat fluxes close to 0, recall from the temperature profiles that small negative fluxes develop later during the night), the top membranes actively lose heat at up to $-15\,W\,m^{-2}$.

3.2. Winter temperature and heat flux profiles

The previous sections analyzed temperature and heat flux profiles for August 2012, a summer month; this section will compare those observations to January 2013, the coldest month of the observational period. The average air temperature in January was 1.3 °C compared to 23.8 °C in August. The timestamps above the plots are here in EST (UTC-0500). Figs. 5 and 6 show monthly-averaged profiles of temperature and heat flux, calculated in identical fashion to the summer months. From the figures, it is clear that the top membrane temperature for all the rooftops averages around 5 °C at 0015, 0415, 0815 and 2015 h, in fact they only change during the midday and afternoon periods (1215 and 1615 h) due to the reduced length of insolation in the winter in Princeton, NJ. During all time periods, there exists a negative gradient between depths 2 and 3, indicating heat transfer from the building into the insulation layers, except at THYb-R3.7 during the midday period. For THYb-R3.7, the profile is inverted at 1215, indicating a downward heat flux in the lower parts of the insulation layer that can be directly attributed to its low insulation thickness allowing the downward heat flux front to reach the bottom within the period where solar radiation is heating the external membrane. However, this downward heat flux in the THYb-R3.7 insulation layer is not translated into heat gains for the indoor space: unlike the warmer month, a transition of the roof from being a sink of heat to being a source never really materializes in the winter months and the buildings are continuously losing energy to the surrounding. This can be concluded by noting that the plenum temperatures (lowest level) remain around 15–22 °C for the buildings, which is higher than the bottom insulation temperature even for THYb-R3.7 at 1215.

Fig. 6 shows the heat flux profiles for January 2013. The midnight and early morning heat flux profiles from January suggest flux homogeneity over the entire roofing depth and the surrounding environment (except for LSBb-R4.2 where the fluxes still vary with depth, albeit mildly). The lack of significant flux gradient indicates that the heat lost at both the top and bottom of the roof is roughly the same for all the structures. This is attributed to the length of the nighttime condition during the winter that allow temperature profiles in the insulation layer to become linear, as revealed in Fig. 5. The influence of insulation is visible in all the subplots: the ADMw-R8.4 consistently experiences the lowest heat transfer compared to all other roof structures at almost all time periods. At midnight, while all other roofs lose around $-4\,W\,m^{-2}$ at the bottom, the heat lost at ADMw-R8.4 roof is half that amount.

It is important to note that the highest energy losses from the top membrane, rather than occurring in the middle of the night, occur in the afternoon around 1615 when the top most layer is losing on average around $-10\,W\,m^{-2}$ at THYb-R3.7, LSBw-R4.2 and EGRb-R6.3, while the LSBb-R4.2 roof is losing around $-15\,W\,m^{-2}$. This sudden increase in upward heat flux at 1615 occurs also in August. Both the summer and winter peaks in upward fluxes at 1615 are due to the decrease in solar radiation coinciding with the peak in surface temperatures that the roofs reach at those times. These factors combine to maximize longwave radiative and convective cooling and to reduce solar radiative gain such that the energy budget of the roof becomes in deficit, and upward flux from the insulation layer is maximized to balance the budget and sustain the surface cooling. But these fluxes do not necessarily translate into upward fluxes at the bottom of the insulation due to the thermal inertia of the layer.

As suggested by the temperature profiles, the fluxes at the bottom of the insulation are always negative, and hence the roof structures acts as a heat sink for the indoor space at all time periods, absorbing thermal energy. The top part of the roof, while mostly losing heat to the exterior, switches to gaining heat during the early morning to midday period where it receives high shortwave solar radiative flux, particularly for black roofs. However, this gain is short-lived and all roofs revert to losing heat at 1615, when strong longwave radiative cooling occurs. The black roofs, THYb-R3.7 and LSBb-R4.2 absorb the most during the mid-day period, 6 and $12\,W\,m^{-2}$, respectively, due to their high peak temperatures.

Comparing the August and January profiles one can note that for the peak cooling loads (peak summertime positive fluxes at the bottom of insulation at 1215 and 1415), the roofs can be clearly segregated based on roof color. For peak heating loads (peak wintertime negative fluxes at the bottom of insulation at 0015 and 0415), the fluxes seem to vary almost linearly with insulation depth

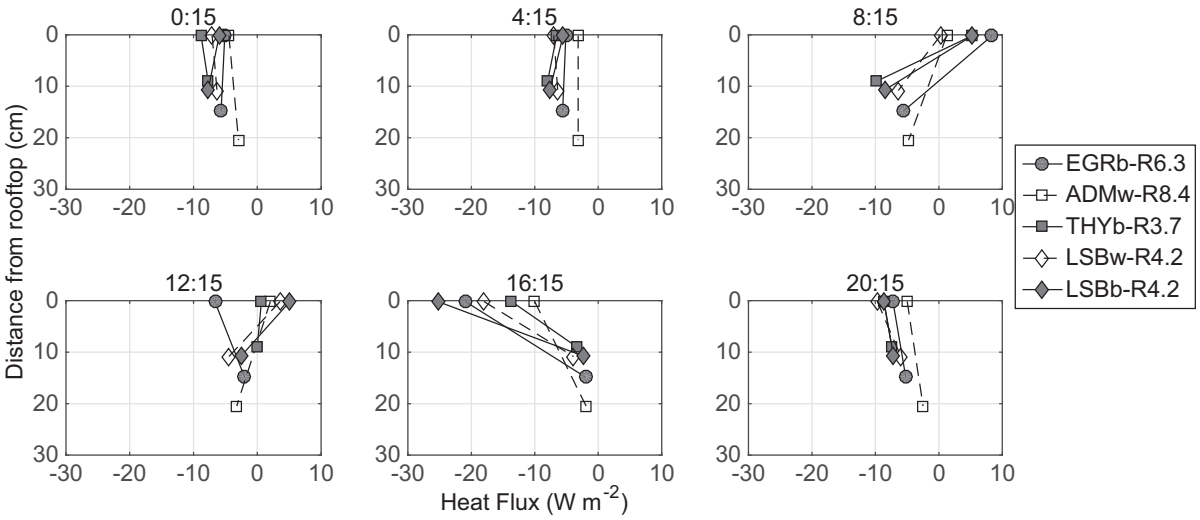

Fig. 6. Averaged heat flux profiles over different roof structures for January 2013.

and roof color plays a minor role. This is expected since roof color has no bearing on the thermal dynamics when there is no solar radiation at night, while it is very important during the solar downwelling radiation daytime peak. These observations are not entirely surprising, but they will be very important later in the discussion so we underlined them here.

3.3. Diurnal variation

To further understand the daily variation of heat flux over various rooftops, the diurnal cycles of 30-min-averaged heat fluxes from the top and bottom plates were averaged for different months. Fig. 7 shows this variation for all roof structures for August 2012. The average daily maximum air temperature during this month was around 30 °C and the average lows were close to 21 °C. The total precipitation was 25 mm. It is obvious from the graph that there exists a difference in amplitude and phase between the heat flux directly under the membrane and the flux at the bottom of the insulation. The black roofs EGRb-R6.3, LSBb-R4.2 and THYb-R3.7 all have peaks around 40–50 W m^{-2}. In stark contrast the white roofs LSBw-R4.2 and ADMw-R8.4 peak at 15–20 W m^{-2}. This dissimilarity observed in the magnitude of heat fluxes is directly related to the difference in albedos. In addition, the higher albedo over white roofs is also responsible for maintaining the heat flux values close to zero when the incoming solar radiation is low. Over the black roofs during the late afternoon hours, while the atmosphere is rapidly cooling, high negative fluxes are observed. Albedo is also responsible for the reduced heat fluxes at the bottom of the roof. While the peak heat flux at the bottom over white roofs average around 2–4 W m^{-2} the heat flux recorded at the bottom of black roofs peak around 12–14 W m^{-2}. But it is interesting to note that even among the heat fluxes observed at the top, the black roofs peak much earlier compared to white ones. The black roofs, at the top, have flux peaks around 0800 EDT, whereas the white roofs peaks around 0930–1000 EDT. As described above, the black roofs peak around 40–50 W m^{-2} and the white roofs peak at much lower value, 15–20 W m^{-2}. This difference in magnitude and phase is directly related to the effect of the roof albedos. Apart from differences in albedo, insulation thickness and ageing of the membrane also contribute to the dissimilarities observed.

The diurnal variations in temperature and heat flux profiles indicate the complex role played by the roof's thermal inertia. While it is evident that the membrane albedo restricts the heat exchanged between the roof and the surrounding environment, insulation thickness plays a crucial role in delaying the transfer of this heat indoors. Fig. 7a and b shows that, while the heat fluxes below the

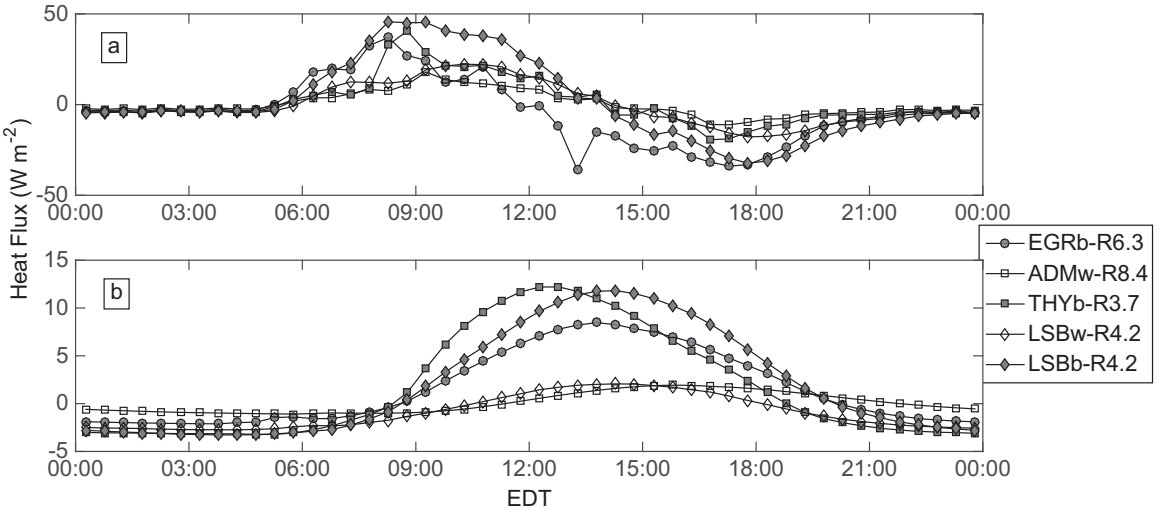

Fig. 7. Averaged diurnal variation of heat flux at the top (top panel) and bottom (bottom panel) of different roof structures for August 2012.

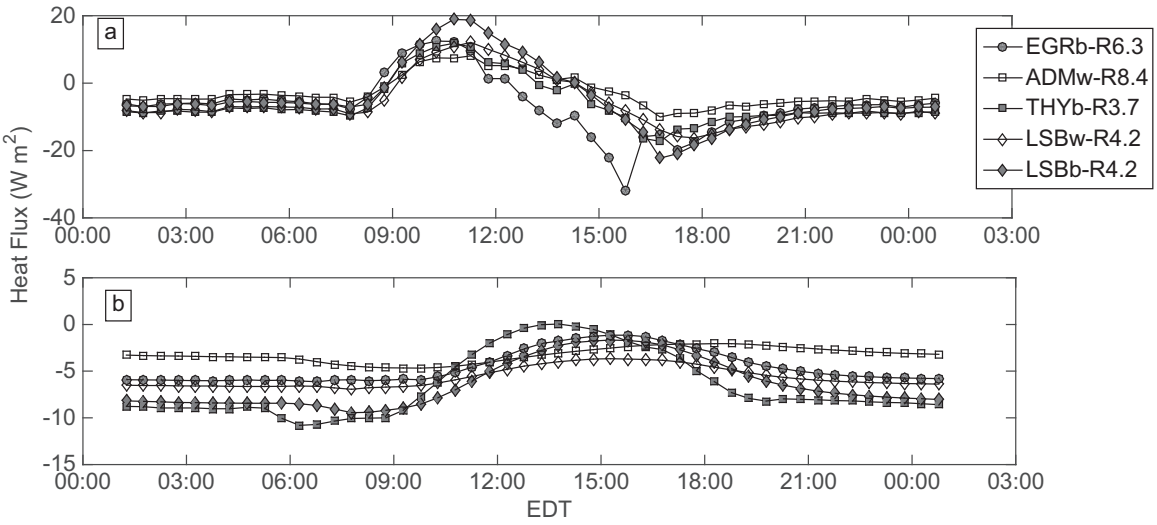

Fig. 8. Averaged diurnal variation of heat flux at top and bottom of different roof structures for January 2013.

membrane peak around 0800–1000 local time, the bottom peaks are delayed by at least 2 h and vary with insulation thickness. The THYb-R3.7 roof peaks around midday, while the other roofs peak during the early afternoon periods. Peak times are quite important since the phase shifts in heat gains over well insulated roofs could be used effectively to spread out the cooling loads more evenly in time by delaying the flux from the roof compared to the flux from windows and from air exchanges (these have the same phase as air temperature, which peaks in the early afternoon).

Fig. 8 describes the monthly averaged diurnal variation of top and bottom heat fluxes for January 2013. During January 2013 the ambient air temperature peaks averaged around 2 °C and the lows averaged around −2.5 °C. As expected during January (Fig. 8), the maximum heat flux values at the top are much lower than during the summer. LSBb-R4.2 peaks are about 18 W m^{-2}; EGRb-R8.4 and THYb-R3.7, the other black roofs, both have peaks around 12 W m^{-2}. The phase difference between top and bottom fluxes is clearly visible and depends on insulation thickness, but not on albedo since the LSBw-R4.2 and LSBb-R4.2 roofs fluxes peak at the same time (around 1100 at the top and 1530 at the bottom). At the bottom, Fig. 8b, the THYb-R3.7 roof, which has the lowest insulation is the only roof structure that exhibits very small positive fluxes during peak insolation time. All other roofs fluxes remain negative, i.e. they continue to cause heat loss from the buildings all day long. As expected, the ADMw-R8.4, which has the highest insulation, allows the least amount of fluxes out and its diurnal cycle remains quite flat, indicating less variability relative to other roof structures.

3.4. Average heat flux

Fig. 9 shows the average energy in kJ m^{-2} day^{-1} that enters (positive) or leaves (negative) the building (bottom of insulation). Data from the bottom-most heat flux plate were integrated over each day and averaged over a whole month to obtain the monthly bar chart of daily heat fluxes. The chart shows that, during the warmer months, August, September, May, June and July the black roofs act as a net source of energy for the indoor space, whereas the white roofs, especially LSBw-R4.2, acts as a net sink. LSBw-R4.2 releases 76, 140, 136 and 14 kJ m^{-2} day^{-1} for August, September, May and June, while ADMw-R8.4 has small net gain during August, June and July (7.6, 10 and 45 kJ m^{-2} day^{-1}, respectively), but acts as a sink in September and May (34 and 53 kJ m^{-2} day^{-1}, respectively). This is very much due to the albedo of the membrane. The LSBw-R4.2 roof was newly laid in Summer 2012 and has an albedo close to 0.55 compared to the older membrane on ADMw-R8.4, which has an albedo around 0.35.

During the colder months, the insulation thickness plays a much more dominant role than albedo. A direct correlation can be seen between the energy lost from the buildings and their *R*-values. The ADMw-R8.4, loses the least amount of energy. In November, the ADMw-R8.4 suffers a net loss of 230 kJ m^{-2} day^{-1} whereas the THYb-R3.7 loses 490 kJ m^{-2} day^{-1}. The LSBw-R4.2 and LSBb-R4.2, the identical new roof structures, lose around 436 and 450 kJ m^{-2} day^{-1}, respectively. The EGRb-R6.3 loses close to 330 kJ m^{-2} day^{-1}. The bars indicate that doubling the insulation almost halves the losses; this is consistent with the fact that the heat flux in the roof *Q*, under steady state conditions, should scale as $Q \sim 1/R$. The plots also show that, as the membrane ages, it loses its effectiveness. The LSBw-R4.2 roof, which is very new, has almost twice the albedo of the ADMw-R8.4 roof.

One surprising finding was that during December, less heat was lost compared to November. A closer inspection of the difference between the indoor temperatures measured at the air plenum and the temperature at the bottom of the insulation foam revealed a

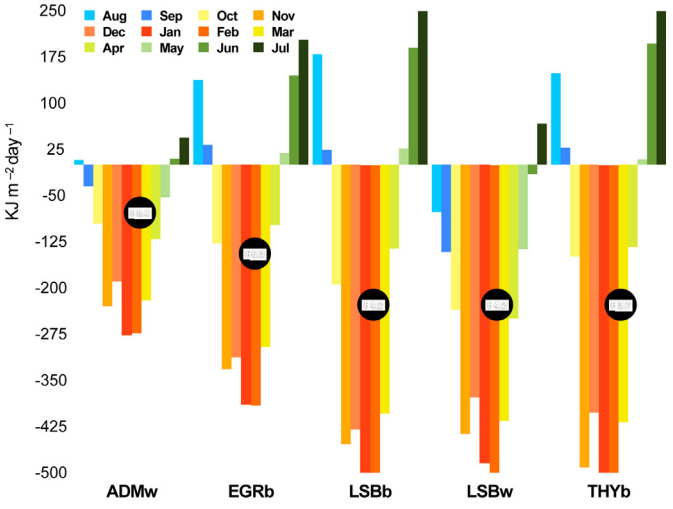

Fig. 9. Averaged daily heat flux in/out of roof structures from August 2012 to July 2013. A positive value indicates heat absorbed by the building while a negative flux indicates heat lost by the building.

higher difference (about 0.5 °C higher) during November compared to December. Given that December was colder (leading to higher temperatures at the bottom of the insulation), this indicates that indoor temperatures remained higher in November. This could either be due to the pronounced entrainment of colder outside air through hallways, doors and windows during December thereby considerably reducing the indoor temperature or due to reduced indoor heating during the Winter break at the end of December.

Finally, it should be noted that aging and temperature do affect the heat flux measured, however it is impossible to attribute the individual contribution of these effects as it requires continuous observation of changes in physical properties (thermal conductivity and thermal capacity of the insulation foam and roof membrane) of the roof material. Nevertheless, while aging and temperature effects reduce the thermal efficiency of the roof structure in moderating the heat entering and leaving the building envelope, the large scale differences noticed here are primarily a factor of insulation thickness and membrane reflectivity. As one can infer from Fig. 9, the LSBw-R4.2 and LSBb-R4.2 roofs which have identical roof insulation and were laid at the same time (Summer 2012), let in the same amount of heat during the winter months (around −450 to −500 kJ m^{-2} day^{-1} for January and February) when the effect of insulation thickness is pronounced, but during the summer months have significantly different values, around 250 kJ m^{-2} day^{-1} for LSBb-R4.2 and kJ m^{-2} day^{-1} for LSBw-R4.2 in July. Furthermore, the ADM and EGR roofs which are older compared to LSBw-R4.2 and LSBb-R4.2 roofs but have higher insulation thickness, let out less heat during the winter months. The ADMw-R8.4 which has an R value of 8.4 let out −275 kJ m^{-2} day^{-1} of heat in December compared to −500 kJ m^{-2} day^{-1} let out by the newly laid LSBw-R4.2 and LSBb-R4.2, both of which have an R value of 4.2. These results indicate that any effects of aging and temperature will only strengthen our argument, as it will widen the difference between the less insulated and more insulated roofs. Finally, while the experimental set up did not account for aging and temperature effects independently, the wide range of insulation and albedo values of the roof structures studied in the experiment, unequivocally proves insulation thickness and albedo as the primary factors in determining the energy entering or leaving the roof top.

4. Summary and conclusions

Detailed experimental measurements inside five roofs with different albedos and insulation R-values were conducted to understand the interacting roles of these two roof characteristics on the building energy performance. The results reveal the complex transient dynamics of heat transfer through heterogeneous roof structures. Apart from the relatively well-understood effects of membrane albedo, the thermal storage capacity of the roof elements also plays a significant role in controlling the transfer of energy through roof structures, and this role is also affected by the roof albedo.

Our results indicate that white membranes are highly effective in reducing the cooling load during the warmer months; insulation thickness (R-values) on the other hand controls the heating loads during winter periods. The observations indicate that doubling the R-value leads to halving the amount of heat transferred, irrespective of the membrane albedo; this is consistent with the fact that heat loss under steady state conditions scale as $1/R$. But at what level this becomes financially ineffective needs to be explored more thoroughly.

Overall, energy offsets related to reduced heating loads by black roofs during winter periods were negligible compared to the cooling load reductions allowed by cool roofs during the summer period, in agreement with previous comparable studies in the region [12]. As indicated above, insulation thickness played a much more direct role in reducing the heating loads during the wintertime. The insulation thickness also modulated the phase of heat transfer in the roof; delaying the fluxes at larger depths compared to fluxes at the top of the roof.

Finally, summarizing our findings leads us to conclude that white/reflective membranes with high R-value should be recommended for the Northeastern US region where our study took place. The insignificant differences observed between the heating loads of white/cool and black roofs during winter months, which we linked here to the negligible impact of albedo during peak heating periods (as opposed to its crucial role during peak cooling), support a broader conclusion that cool roofs can help reduce building energy consumption in many cold climate areas that have much higher heating degree days than cooling degree days, which is the case for our study area (heating degree days are almost 5 times the cooling degree days in Princeton, NJ). The white membranes, apart from reducing the cooling load in summer months, will also be beneficial in reducing ambient urban temperatures in dense urban neighborhoods and could be a potential mitigation strategy in reducing the effects of urban heat islands and urban heat stress. This is particularly important given the potential for synergistic interactions between urban heat islands and heat waves, the later being expected to exacerbate due to global warming, which can pose significant health hazards for urban residents [24].

While this article dealt exclusively with the observations made at our field site, in the next part of this study, the results from this analysis will be used to validate a vertically-resolved roof model, PROM (Princeton Roof Model). The model will then be applied to explore a broader mix of R-values and albedos and to address some of the unanswered questions from this study, including at what R-value does the energy transfer plateau? Furthermore, a detailed cost-benefit analysis will be carried out in parallel to energy savings.

Acknowledgements

This work was supported by the U.S. Department of Energy through Pennsylvania State University's Energy Efficiency Building Hub under grant No. DE-EE0004261 and by the Helen Shipley Hunt Fund through Princeton University. The authors also extend their gratitude to the staff members at PPPL for their invaluable help in setting up the experiment.

References

[1] Division of Energy Efficiency and Renewable Energy, 2011 Buildings Energy Data Book, US Department of Energy, 2011.
[2] S.J. Konopacki, H. Akbari, Measured energy savings and demand reduction from a reflective roof membrane on a large retail store in Austin, in: LBNL-47149, Lawrence Berkeley National Laboratory, 2001.
[3] H. Akbari, R. Levinson, Evolution of cool-roof standards in the US, Adv. Build. Energy Res. 2 (1) (2008) 1–32.
[4] M. Santamouris, Cooling the cities—a review of reflective and green roof mitigation technologies to fight heat island and improve comfort in urban environments, Sol. Energy 103 (2014) 682–703.
[5] T. Xu, J. Sathaye, H. Akbari, V. Garg, S. Tetali, Quantifying the direct benefits of cool roofs in an urban setting: reduced cooling energy use and lowered greenhouse gas emissions, Build. Environ. 48 (Feb) (2012) 1–6.
[6] E. Orbendorfer, J. Lundholm, B. Bass, R. Coffman, H. Doshi, N. Dunnett, S. Gaffin, M. Köhler, K. Liu, B. Rowe, Green roofs as urban ecosystems: ecological structures, functions, and services, BioScience 57 (10) (2007) 823.
[7] H. Akbari, M. Pomerantz, H. Taha, Cool surfaces and shade trees to reduce energy use and improve air quality in urban areas, Sol. Energy 70 (Jan (3)) (2001) 295–310.
[8] D.J. Sailor, A green roof model for building energy simulation programs, Energy Build. 40 (Jan (8)) (2008) 1466–1478.
[9] A. Pasupathy, L. Athanasius, R. Velraj, R.V. Seeniraj, Experimental investigation and numerical simulation analysis on the thermal performance of a building roof incorporating phase change material (PCM) for thermal management, Appl. Therm. Eng. 28 (Apr (5)) (2008) 556–565.

[10] H.F. Castleton, V. Stovin, S.B.M. Beck, J.B. Davison, Green roofs; building energy savings and the potential for retrofit, Energy Build. 42 (10) (2010) 1582–1591.
[11] M. Çelebi, H.-P. Liu, Before and after retrofit – response of a building during ambient and strong motions, J. Wind Eng. Ind. Aerodyn. 77–78 (1998) 259–268.
[12] S.R. Gaffin, M. Imhoff, C. Rosenzweig, R. Khanbilvardi, A. Pasqualini, A.Y.Y. Kong, D. Grillo, A. Freed, D. Hillel, E. Hartung, Bright is the new black—multi-year performance of high-albedo roofs in an urban climate, Environ. Res. Lett. 7 (Mar (1)) (2012) 014029.
[13] R. VanCuren, The radiative forcing benefits of 'cool roof' construction in California: quantifying the climate impacts of building albedo modification, Clim. Change 112 (Sep (3)) (2011) 1071–1083.
[14] P. Mukhopadhyaya, M.T. Bomberg, M.K. Kumaran, M. Drouin, J.C. Lackey, D. van Reenen, N. Normandin, Long-term thermal resistance of polyisocyanurate foam insulation with gas barrier, in: Proceedings of the IX International Conference on Performance of Exterior Envelopes of Whole Building, Clearwater Beach, Florida, USA, 2004, pp. 1–10.
[15] R.T.A. Prado, F.L. Ferreira, Measurement of albedo and analysis of its influence the surface temperature of building roof materials, Build. Environ. 37 (4) (2005) 295–300.
[16] H. Akbari, A. Berhe, R. Levinson, S. Graveline, K. Foley, A. Delgado, R. Paroli, Aging and Weathering of Cool Roofing Membranes, University of California, California, 2005 Aug, pp. 1–15 (eScholarship).
[17] M. Bomberg, A model of aging for gas-filled cellular plastics, J. Cell. Plast. 24 (4) (1988) 327–347.
[18] M. Bomberg, D.A. Brandreth, Evaluation of Longterm Thermal Resistance of Gas-Filled Foams: State of the Art, second ed., American Society for Testing and Materials, Philadelphia, PA, 1990, pp. 156–173.
[19] S.K. Meyn, T.R. Oke, Heat fluxes through roofs and their relevance to estimates of urban heat storage, Energy Build. 41 (7) (2009) 745–752.
[20] F. Ingelrest, G. Barrenetxea, G. Schaefer, M. Vetterli, O. Couach, M. Parlange, SensorScope, ACM Trans. Sens. Netw. 6 (2) (2010) 1–32.
[21] Z. Wang, E. Bou-Zeid, J.A. Smith, A coupled energy transport and hydrological model for urban canopies evaluated using a wireless sensor network, Q. J. R. Meteorolog. Soc. 139 (675) (2013) 1643–1657.
[22] A. Desjarlais, T. Petrie, W. Miller, R. Gillenwater, D. Roodvoets, Evaluating the energy performance of ballasted roof systems, in: Presented at the Third International Building Physics Conference, Montreal, 2006.
[23] C.P. Hedlin, Calculation of Thermal Conductance Based on Measurements of Heat Flow Rates in a Flat Roof Using Heat Flux Transducer, American Society for Testing and Materials, Philadelphia, PA, 1985 Feb, pp. 1351.
[24] D. Li, E. Bou-Zeid, Synergistic interactions between urban heat islands and heat waves: the impact in cities is larger than the sum of its parts, J. Appl. Meteorol. Climatol. 52 (Oct (9)) (2013) 2051–2064.